Impact of *in situ* oxygen plasma cleaning on the resistance of Ru and Au-Ru based rf microelectromechanical system contacts in vacuum

M. Walker,[1] C. Nordquist,[2] D. Czaplewski,[2] G. Patrizi,[2] N. McGruer,[3] and J. Krim[4,a)]
[1]*Department of Materials Science and Engineering, North Carolina State University, Raleigh, North Carolina 27695, USA*
[2]*Sandia National Laboratories, Albuquerque, New Mexico 87185, USA*
[3]*Department of Electrical and Computer Engineering, Northeastern University, Boston, Massachusetts 02115, USA*
[4]*Department of Physics, North Carolina State University, Raleigh, North Carolina 27695, USA*

(Received 7 August 2009; accepted 25 January 2010; published online 28 April 2010)

Contact resistance measurements are reported for radio frequency microelectromechanical system switches operating in an ultrahigh vacuum system equipped with *in situ* oxygen plasma cleaning capabilities. Ru-based contacts were prepared by means of standard sputtering techniques, sputtering followed by postdeposition oxidation, (surface RuO_2) or reactive sputtering in the presence of oxygen (bulk RuO_2). *In situ* oxygen plasma cleaning lowered the resistance of Ru contacts by two or more orders of magnitude but not lower than Au contacts, irrespective of whether the Au contacts were cleaned. The time dependence of the resistance was fit to power law extrapolations to infer contact creep properties and resistance values at $t=\infty$. Time-dependent creep properties of mixed Au-Ru contacts were observed to be similar to those of Au-Au contacts, while the absolute value of the resistance of such contacts was more comparable to Ru-Ru contacts. Prior to, and for short oxygen plasma exposure times, bulk RuO_2 resistance values exhibited much larger variations than values measured for surface RuO_2. For O_2 plasma exposure times exceeding about 5 min, the bulk and surface RuO_2 resistance values converged, at both $t=0$ and $t=\infty$, with the $t=\infty$ values falling within experimental error of theoretical values predicted for ideal surfaces. The data strongly support prior reports in the surface science literature of oxygen plasma induced thickening of oxide layers present on Ru surfaces. In addition, they demonstrate that vacuum alone is insufficient to remove contaminants from the contact surfaces and/or prevent such contaminants from reforming after oxygen plasma exposure. © *2010 American Institute of Physics*.
[doi:10.1063/1.3353991]

I. INTRODUCTION

Radio frequency microelectromechanical system (rf MEMS) switches have many promising advantages over solid state switches, particularly with respect to cutoff frequency, insertion loss, linearity, and power consumption characteristics.[1,2] Gold is often used for rf MEMS contacts because of its chemical inertness and low resistivity but its softness resulted in insufficient reliability for commercial applications.[3] Prior studies of gold contacts have been performed in air, nitrogen, or vacuum environments that ranged in pressure from 10^{-3} to 10^{-7} Torr.[4–8] Since these studies were performed in conditions where condensation of contaminants can easily occur, their reproducibility is uncertain. However, if the operating conditions are sufficiently controlled and monitored, as is the case here, the results should be reproducible irrespective of the environment or facility where the measurements are performed.

The use of materials other than gold is necessary for improved reliability and a better understanding of the mechanisms causing premature failure is necessary. Molecular dynamic simulations for both Au and Ru contacts have been studied to understand the ductile and brittle nature of these contacts at different operating temperatures.[9] Ruthenium contacts are a promising alternative to gold[3,9–12] but the conditions under which Ru can be meaningfully studied are more stringent than those required for gold. In particular, Ru is more sensitive to surface contamination by oxygen and hydrocarbon film species than Au.[13] When Ru is oxidized, it has a stable conducting oxide.[14] Iwasaki *et al.*[15] have reported that Ru becomes RuO_2 when exposed to O_2 plasma at room temperature for sufficiently long periods. In addition, they report that RuO_2 is somewhat less conductive than Ru, with bulk resistivity values for Ru and RuO_2, respectively, of 12.3 and 45.0 $\mu\Omega$ cm.[15]

The measurements reported here were performed to (1) document the impact of oxygen plasma on the resistance of Ru-based contacts and to (2) compare the properties of soft, hard, and combined soft-hard contacts for Au-Au, Ru-Ru, and Au-Ru-based contacts. Oxygen plasma was selected as the cleaning method, as it has recently been demonstrated to be far more effective at cleaning occluded areas and high aspect ratio regions than UV ozone.[16] It is thus well suited for cleaning the overhangs and nonline-of-sight regions that are characteristic of rf MEMS switch contacts. It does, however, expose the surface to "oxygen contamination," so that an oxide, rather than pure Ru is to be expected at the surface. In order to compare resistance data for various material com-

a)Electronic mail: jkrim@unity.ncsu.edu.

TABLE I. Theoretical values for the contact resistance. The theoretical values for the surface contact for Au-Au, Ru-Ru, and RuO_2-RuO_2 are calculated using Eq. (2), and listed in the upper portion of the table for realistic upper and lower values of contact radii. The lower portion of the table presents theoretical resistance contributions across the contact pad themselves for Au, Ru, and RuO_2, using $R=\rho l/(\pi a^2)$. The sum of the surface contact resistance and the resistance through the contact is the approximate theoretical resistance, R_T, of the entire contact with no contamination contributions and is shown in Table II.

Theoretical contact resistance			
Contact material	Bulk resistivity, ρ ($\mu\Omega$ cm)	$R=\rho/(2a)$, $a=0.098$ μm (Ω)	$R=\rho/(2a)$, $a=0.68$ μm (Ω)
Au-Au	2.44	0.124	0.018
Ru-Ru	12.3	0.628	0.090
RuO_2-RuO_2	45	2.296	0.331
Theoretical resistance through a contact pad			
	Ru film thickness	$R=\rho l/\pi a^2$ (Ω)	$R=\rho l/\pi a^2$ (Ω)
Ru	$l=181$ nm	0.738	0.0153
	RuO_2 film thickness	$R=\rho l/\pi a^2$ (Ω)	$R=\rho l/\pi a^2$ (Ω)
RuO_2	$l=6$ nm	0.0895	0.0019
	$l=187$ nm	2.796	0.058

binations, time-dependent resistance measurements were performed for closed contacts for 30 min periods, both before and after cleaning. The data were fit to power law extrapolations to infer contact creep properties and $t=\infty$ resistance values. In the following sections, a brief discussion of ideal contact resistance and its time evolution is first presented, following by a presentation of the experimental results

II. IDEAL CONTACT RESISTANCE AND CONTACT CREEP THEORY

The apparent contact area of an rf MEMS switch is typically 3 to 20 μm^2, while the actual area in contact may be only 100th as large, typically in the range of $0.003-1.4$ μm^2.[16] This arises from the fact that only the outermost asperities of the contacting surfaces are actually touching.

The contact resistance R_C for one individual asperity contact can be written as

$$R_C = f\left(\frac{\lambda}{a}\right)R_M + R_S = \frac{1+0.83(\lambda/a)}{1+1.33(\lambda/a)}\frac{\rho}{2a} + \frac{4\rho\lambda}{3\pi a^2}, \quad (1)$$

where a is the asperity contact radius, ρ is the resistivity, and λ is the electron mean free path.[17–19] R_M is the "Maxwell" resistance associated with lattice scattering of electrons. It dominates when the asperity contact size is much larger than the electron mean free path. R_S is the "Sharvin" resistance associated with boundary scattering of the electrons. It dominates when the asperity contact size is on the order of the electron mean free path. The interpolation function $f(\lambda/a)$ allows for a smooth transition between resistance regimes. It has a maximum value of 1 for $a \gg \lambda$ and a minimum value of 0.624 for $a \ll \lambda$. An upper limit of contact resistance R_U can be estimated by summing individual asperity contact areas together, yielding a single contact with an effective radius a_{eff}, which is the limiting case of the first term in Eq. (1).

$$R_U = \frac{\rho}{2a_{eff}}. \quad (2)$$

Equation (2) generates an effective radius in the range of $0.098-0.68$ μm, for actual contact areas ranging from $0.03-1.4$ μm^2. This is much larger than the electron mean free path for any of the materials studied here (38, 1.97, and 3.32 nm, for Au, Ru, and RuO_2, respectively).[15,20]

Actual contact area increases in time if the surfaces are held together, by approximately 1% after a closure time of 1 s to approximately 7% after a closure time of 40 h (Ref. 15), depending on the physical properties of the materials in contact. The nature of the contact obviously controls the contact resistance, and the time dependence of the resistance of the contact reflects its materials properties. For Au switches, it has been shown both theoretically and experimentally that the time dependence of the resistance follows a power law relation:[17]

$$R(t) = At^{-\alpha} + B, \quad (3)$$

where A reflects the topography of the contacts and increases with roughness, α is an intrinsic material property related to material creep properties[17] and B is a theoretical limiting resistance at $t=\infty$. For the conceptual case where $t=\infty$, B corresponds to the resistance after all asperities have been flattened into one short and cylindrical wire. The cross sectional resistance of a wire is $R=\rho l/\pi a^2$, where l is the length of the wire.

Ideal values for the resistance of Au, Ru, and RuO_2 contacts are listed in Table I. The values in Table I are calculated using Eq. (2), and listed in the upper portion of the table (a) for realistic upper (0.68 μm) and lower (0.098 μm) values of effective contact radii. The lower portion of the table pre-

TABLE II. Fit parameters for Eq. (3), the power law fit and the error of the line to data. The limiting resistance for O_2 plasma cleaning, B, which is an extrapolation of the actual contact resistance if the contact remained closed forever, favorably agrees with calculated contact resistances in Table I. The last column is the sum of the surface contact resistance and the resistance across the contact pad in Table I for $a=0.68$ μm (or 7% of the real contact area).

Contacts	α	A (Ω/min$^{\alpha}$)	B (Ω)	Line fit error R^2
Au-Au pre O_2 cleaning	0.0351	1.01	0.01091	0.99286
Ru-Ru pre O_2 cleaning	0.08758	197.61	3.00372	0.99658
Ru-Ru post O_2 cleaning	0.01312	6.53	0.62073	0.97697
Au-RuO_2 post O_2 cleaning	0.01946	8.87	0.04489	0.98769

sents theoretical resistance contributions for the resistance across the contact pad themselves for Au, Ru, and RuO_2, using $R=\rho l/(\pi a^2)$.

The sum of the surface contact resistance and the resistance through the contact is the approximate theoretical resistance, R_T, of the entire contact with no contamination contributions and is shown in Table II.

III. EXPERIMENTAL SETUP

Four point resistance measurements were taken for all contacts. Measurements were recorded on switches designed and fabricated at either Northeastern University (NEU) or Sandia National Laboratories (SNL). The physical configuration of the NEU switch design has been reported earlier and Fig. 1(a) is an image of the switch.[21] NEU switches were released and wirebonded at NEU. There is only one sense pad for each switch, so that the sense and source connections for four wire resistance measurements are connected externally to the chamber. There are two dedicated wirebonds on the die for the ground connections for the four wire resistance measurements. These switches are comprised of either sputtered Au-Au or sputtered Ru-Ru contacts. Switches on all die were held to the underlying ceramic packages by the wirebonding wire, i.e., without the use of an adhesive.

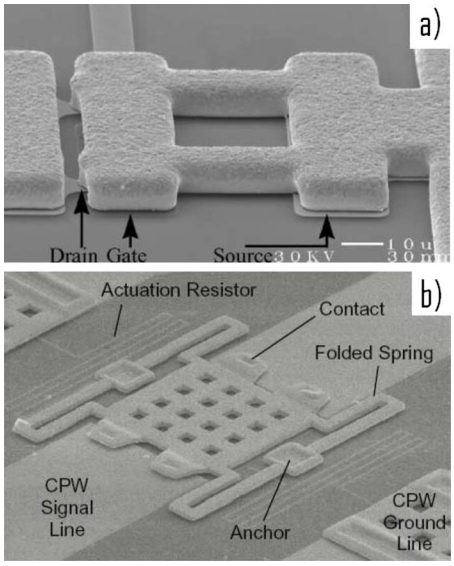

FIG. 1. (Color online) Scanning electron microscopy images of (a) NEU rf MEMS device (Ref. 21) and (b) SNL rf MEMS device (Ref. 23).

The SNL switches were fabricated, released, and wirebonded at SNL and Fig. 1(b) is an image of the switch.[22] Each die consists of 12 switches that are divided into three isolated banks of four. Each bank of four switches share two common ground pads, one sense pad and one source pad to enable four wire resistance measurements at the switch itself. Each device has a dedicated actuation pad to close specific switches. Each ground pad is wirebonded to the package bottom to mitigate electrostatic discharge. All top contacts are Au while the bottom contacts are reactively sputtered RuO_2 (bulk RuO_2) or sputtered Ru that is oxidized after deposition (surface RuO_2). The thicknesses of the Ru contacts are 181 nm. The surface RuO_2 is an additional 6 nm thick. Each die has at least four bulk and four surface RuO_2 contacts. The NEU and SNL switches were both wirebonded with one mil (25 μm) Au wire to unlidded 24 pin or 40 pin side braze ceramic dual inline package (DIP) contact pads. They were transported in ambient to North Carolina State University (NCSU) in ESD protective packages and held in place by pressing the leads into an ED resistant form. At NCSU, they were stored for periods ranging from days to months, in a N_2 filled glove box in advance of the measurements. The studies reported here do not rule out the possibility that thicker contamination films were present on switches stored for longer periods of time.

Figure 2 was the chamber used for these experiments. The MEMS stage consists of two custom built rectangular machinable glass ceramic pieces with an array of holes drilled out to support 24, 40, and 64 pin side braze DIP. These ceramic pieces were mounted on oxygen-free high-conductivity Cu that was suspended inside the chamber. All pin sockets were connected to standard vacuum wires by spot welding, to reduce the possibility of outgassing in vacuum and during plasma cleaning. Two Cu disks, 2.5 in. diameter and 0.25 in. thick, were mounted on either side of the MEMS stage and were connected to a high voltage power supply for generating plasma *in situ*.

IV. DATA COLLECTION AND RESULTS

Experimental resistance values were measured using a four probe resistance technique, sourcing 0.02 V with a compliance current of 0.02 A, Ref. 23. This includes resistance from the signal lines, the device contact pads and any additional resistances from contaminants that are potentially present on the contact pads. In order to quantify the addi-

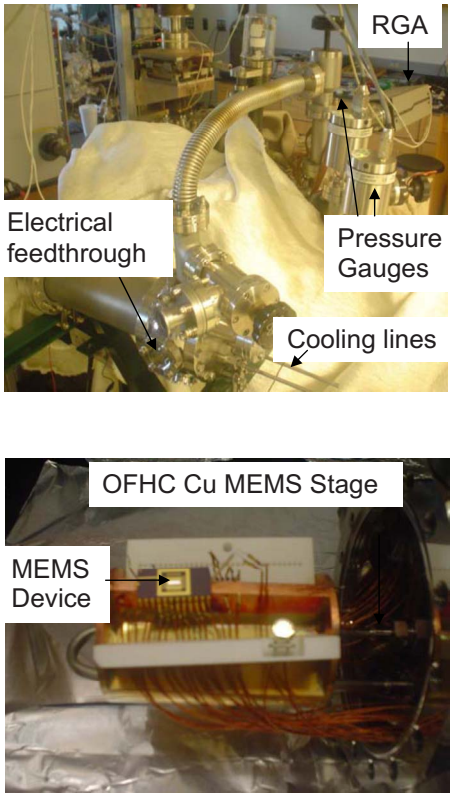

FIG. 2. (Color online) Photographs of experimental chamber.

tional resistance in the connection lines for NEU switches, the four wire resistance of the ground connections was measured, and it was then assumed the sense and source connections were similar. Values reported here have been corrected for the resistance in the connection lines. Once the switch was closed, a four wire dc contact resistance measurement was performed across the contact with a Keithley[22] source meter.

The actuation voltage to close NEU switches ranged from 85–95 V, corresponding to 50 to 100 μN, and for SNL switches, it from 87 to 99 V, corresponding to 280 to 365 μN.[21,23] Once any device was closed, the actuation voltage was held constant until the switch was opened by removing the actuation voltage. The actuation voltage was supplied by an Agilent waveform generator[24] through a TEGAM high voltage amplifier[25] to the appropriate actuation switch pad. To verify the actuation voltage, a monitoring output from the TEGAM was measured by a Keithley[26] multimeter. LABVIEW was used to collect all data and enter all input parameters.

After mounting the ceramic package in the vacuum chamber, the chamber was evacuated to a base pressure of 1×10^{-9} Torr. Oxygen plasma cleaning treatments were performed as follows: all actuation voltage and four wire resistance connections outside the chamber were disconnected from the feedthroughs and a gate valve, which connected the sample chamber to the ion pump was then closed. Research grade O_2 was leaked into the sample chamber until the Baratron capacitance manometer pressure gauge read approximately 150 mTorr. To maintain 150 mTorr pressures, the system was simultaneously pumped with a turbo molecular pump that was gated to maintain 150 mTorr. One Cu disk

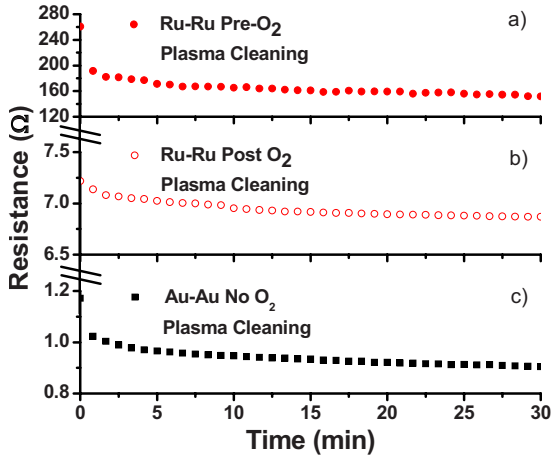

FIG. 3. (Color online) Resistance vs time for switches held closed for 30 min. (a) NEU Ru-Ru switch in 10^{-9} Torr, (b) after exposure to O_2 plasma for one minute, and (c) NEU Au-Au switch in 10^{-9} Torr. Resistance values for cleaned Ru-Ru switches remain higher than Au switches that have not been cleaned.

was connected to a potential of 0.4 kV, while the remaining Cu disk and body of the vacuum chamber was connected to the ground of the power supply.

Initial measurements of the impact of oxygen plasma on Ru-Ru switches were first performed, via comparisons of NEU Ru-Ru and Au-Au resistance data. Given that Ru surfaces, while being cleaned by the oxygen plasma, were also oxidized by it, more extensive studies of switch response were reserved for the combined Au-RuO_2 SNL switches.

A. NEU Ru-Ru and Au-Au comparisons

Figure 3 presents resistance versus time data for NEU Ru-Ru switches held closed for 30 min before (a) and after (b) one minute of exposure to O_2 plasma. Both the switch and contact were composed of sputtered Ru. The base pressure in the chamber before cleaning were 1×10^{-9} Torr. Data was recorded at a chamber pressure of 10^{-8} Torr after cleaning. Cleaning the Ru contacts lowered the resistance by a factor of 20 and was attributed to the removal of hydrocarbons from the surface. For comparison purposes, data for NEU Au-Au switches held closed in 10^{-9} Torr with no cleaning treatment are presented in Fig. 3(c). Resistance values recorded on the NEU Au contacts were similar to those reported in Ref. 8 and fit well to the power law relation expressed in Eq. (3), albeit with different power law parameters. The difference may be attributed to the superior vacuum conditions at which the present studies were performed. Despite the fact that *in situ* oxygen plasma cleaning dramatically lowered the resistance of Ru contacts, it did not lower the resistance to values lower than those characteristic of Au contacts, irrespective of whether the Au contacts were cleaned. The power law fit parameters for the Fig. 3 data are presented in the upper three rows of Table II.

B. SNL bulk and surface oxide comparisons

As a follow up to the initial measurements of NEU Au-Au and Ru-Ru switch response to oxygen plasma, the impact of *in situ* cleaning on SNL Au-RuO_2 switches was

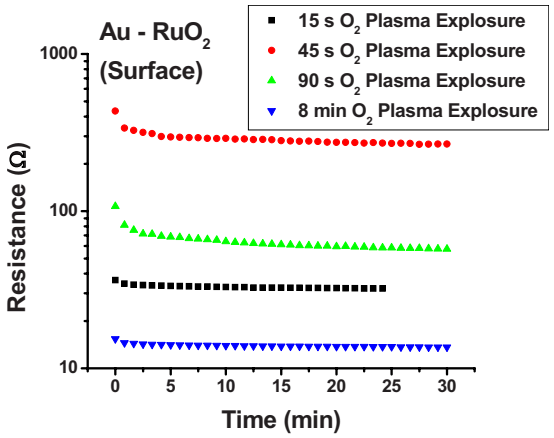

FIG. 4. (Color online) Au-surface RuO_2 contacts from SNL operated in vacuum after O_2 plasma exposure of 15 s, 45 s, 90 s, and 8 min.

studied. The motivation was to compare oxygen plasma exposure for "bulk" and "surface" Ru oxides in controlled conditions, as well as to document the impact of a mixed soft-hard Au-Ru contact. Data were recorded on numerous "surface" and "bulk" RuO_2 switches as a function of oxygen plasma exposure periods. In addition, baseline measurements on the same switches were performed in air and in base level vacuum before the oxygen plasma treatment and in vacuum eight days after the treatment. Figures 4 and 5, respectively, present representative data for an individual switch, and the average results with error bars for the entire collection studied.

Figure 4 presents typical data for a Au-"surface" Ru oxide switch that was held closed for 30 min. The measurements were recorded after 15 s, 45 s, 90 s, and 8 min of O_2 plasma exposure. The base pressure in the chamber before cleaning was 1×10^{-9} Torr and data were recorded at a chamber pressure of 10^{-8} Torr. The resistance measurements increased for contacts exposed to O_2 plasma for 45 s compared with 15 s, but for longer O_2 plasma exposure times (90 s and 8 min), the resistance dropped below initial values because all hydrocarbons have been removed and only the surface oxide layer remains. The increase in resistance for 45 s plasma cleans was thought to be a convolution of partial removal of hydrocarbons on the surface with the initial stages or thickening of an oxide layer forming on the surface.

Figure 5 presents collective data for many switches and runs. In particular, it shows the average values for initial and $t=\infty$ resistance values as a function of oxygen plasma exposure time. The data reflect multiple "surface" and "bulk" RuO_2 switches. Overall, while a variability was present in the data at the initial times, probably due to surface contamination, after about 5 min of exposure to oxygen plasma the data sets converge at both initial and $t=\infty$ time periods. There are no values for 15 s O_2 plasma exposures of bulk RuO_2 because these contact closures could not be fitted by a power law relation. Initial resistance values were on the order of 100 s of kΩ. for these samples and they exhibited far more variability in their initial values than the "surface" Ru samples. As the switches were exposed to longer O_2 plasma times, all resistance measurements exhibit power law trends and both initial and infinity contact resistance values de-

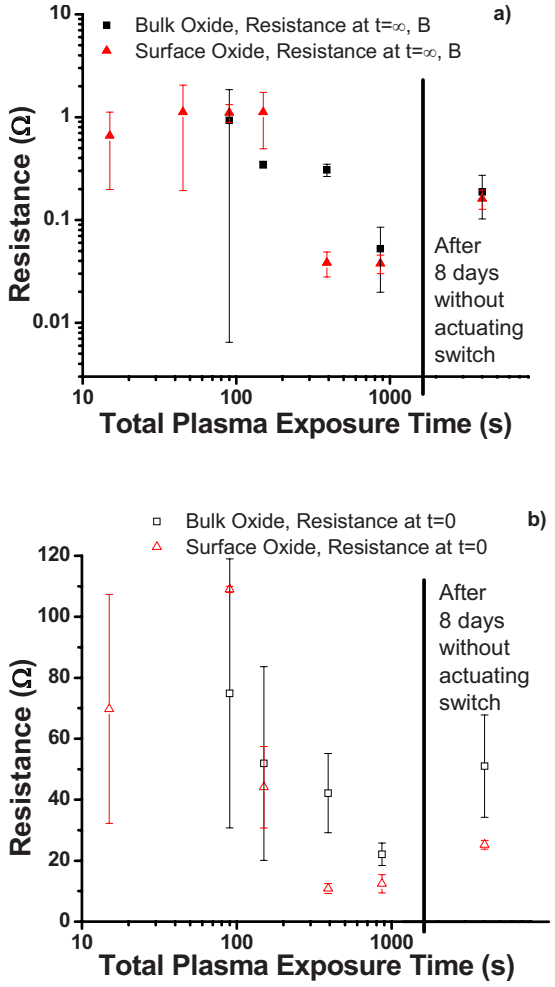

FIG. 5. (Color online) Resistance measurements vs variable exposure times showing that longer exposure times decreases both (a) $t=\infty$ resistance and (b) initial resistance values. The solid black line represents a break in the time axis in order to show switch response after left for eight days in the open position in 10^{-8} Torr vacuum. Vacuum conditions thus failed to prevent the slow reformation of adsorbed species on the surfaces of the cleaned switches.

creased. The power law fit parameters for Au-RuO_2 contacts from Fig. 4 after exposure to O_2 plasma for 8 min are presented in the fourth row of Table II.

The last set of data points in Fig. 5 are measurements of contact resistance after the switches were left for eight days in vacuum at 10^{-8} Torr in the open position. The increase in both initial and limiting resistance can be attributed to slowly forming surface contamination. At 10^{-8} Torr, approximately 0.01 monolayer/s could strike the surfaces, some of which may adsorb and cause an increase in resistance.

V. DISCUSSION

Figure 6 displays normalized resistance changes recorded for Au-Au, Ru-Ru, and Au-RuO_2, where it is clear that the time evolution of the Au-RuO_2 contact is very similar to that of the Au-Au contacts. This is consistent with prior literature reports of creep rate[27] elasticity,[28] contact melting,[29] friction,[30,31] and energy dissipation[32] being dominated by the more compliant material. A slower rate of contact resistance change was anticipated for the Ru-Ru combi-

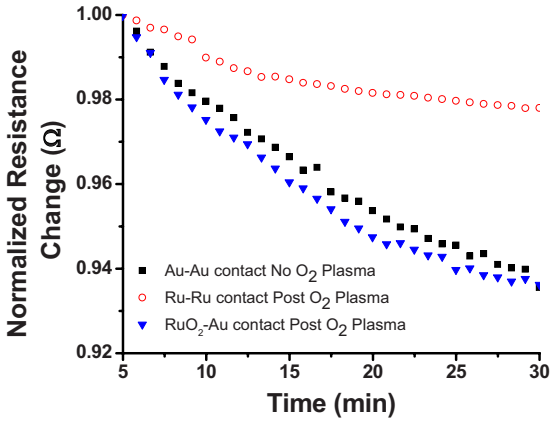

FIG. 6. (Color online) Normalized resistance change of Au-Au, Ru-Ru, and RuO_2-Au contacts. Symbols match prior figures: Ru-Ru [Fig. 3(b)] and Au-Au [Fig. 3(c)]. The Au-Au contacts were not exposed to O_2 plasma. Ru-Ru contacts were exposed to O_2 plasma for 1 min. Au-RuO_2 contacts were exposed to O_2 plasma for 8 min. Au-RuO_2 contacts have similar resistance changes as Au-Au contacts and faster than Ru-Ru contact resistance changes.

nation, as Ru resists deformation more than Au, as observed here. The absolute value of the resistance for the mixed material contact in Fig. 4, meanwhile, remains closer to that of the higher resistance material Ru-Ru contacts in Fig. 3. Table II shows the power law fit parameters of three closures in Fig. 3 plus an additional Au-RuO_2 contact closure of post O_2 cleaning. The limiting resistance B values compare favorably with the theoretical values in Table I.

The schematic in Fig. 7 depicts how the SNL surface and bulk RuO_2 films are thought to evolve and converge as a function of oxygen plasma exposure time. The NEU Ru-Ru contacts would be represented by surface RuO_2 in Fig. 7 but with a thinner oxide layer than SNL surface RuO_2. Using this schematic as a guide, tabulated calculations are presented in Table I for ideal contact resistance of Au, Ru, and RuO_2 contacts. Two resistance measurements were calculated, contact area with radius a and the thickness of the material with length l. The values for l were taken from SNL contact deposition parameters, while a was taken from approximations based on computational values of apparent areas.[17]

Fortini *et al.*[9] used molecular dynamic simulations to study contact closure and opening of Au-Au and Ru-Ru at different temperatures. At their respective elevated temperatures, 300 K for Au and 600 K for Ru, contacts were more

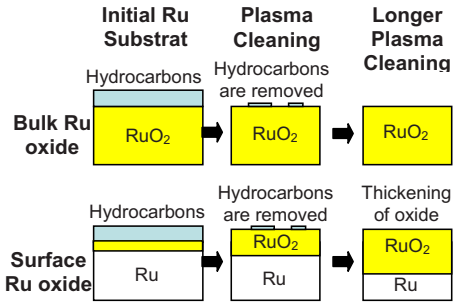

FIG. 7. (Color online) A representation of the bulk and surface RuO_2 initially and when exposed to O_2 plasma for short and long periods of time. Note this is not to scale.

ductile and show necking when pulled apart. At their respective lower temperatures, 150 K for Au and 300 K for Ru, both contacts are brittle and form more dislocations and cracking formation when pulled apart. Using Wiedemann–Franz principle to estimate experimental contact temperatures at voltage values of 0.02 V, the contacts were assumed to be ~300 K. At this temperature the Au-RuO_2 contact had a ductile Au contact with a brittle RuO_2 contact, assuming RuO_2 response similarly as Ru. It was also assumed that RuO_2 would not crack when in contact with Au because Au would deform more easily when pulled apart from RuO_2. This was believed to be seen in Fig. 6 with Au-Au and Au-RuO_2 contacts having similar resistance changes over time. Here, the change in Au was much faster than Ru, as shown by Fortini as being more ductile, so that faster resistance change was dominated by the material that had an increased contact area, consistent with the present set of experimental observations.

This work has shown that for a sufficiently long O_2 plasma exposure time, the contact resistance can decrease by a factor of 20, which is consistent with removal of contaminants that were not removed by vacuum conditions alone. No evidence for plasma-induced changes in roughness were observed.[33–36] Prior to, and for short oxygen plasma exposure times, bulk RuO_2 resistance values exhibited much larger variations than values measured for surface RuO_2, which can be attributed to a higher degree of susceptibility to physisorbed hydrocarbons that are not removed by vacuum conditions (10^{-8} Torr) alone. The fact that exposing contacts to 10^{-8} Torr vacuum for several days causes the contact resistance of cleaned switches to increase demonstrates that the vacuum conditions in addition could not preserve the cleanliness of the switches for extended periods. This leads to questions about how to keep the contact resistance from gradually increasing over the lifetime of a packaged rf MEMS switch. One suggestion would be after cleaning the contacts, backfill, and seal a nonreactive gas into the packaging of the device and/or store the switches with the contacts in a closed position. This could limit the probability of reactive hydrocarbons from interacting with the contacts thereby keeping the contact resistance low.

VI. SUMMARY

A series of experiments was performed to investigate the time evolution of contact resistance for soft (Au), hard (Ru), and a combination of soft and hard metal contacts for rf MEMS switches operating in an ultrahigh vacuum system equipped with *in situ* oxygen plasma cleaning capabilities. Ru-based contacts were prepared by means of standard sputtering techniques, sputtering followed by postdeposition oxidation, (surface RuO_2) or reactive sputtering in the presence of oxygen (bulk RuO_2). The time dependence of the resistance was fit to power law extrapolations to infer contact creep properties and to infer limiting resistance values at $t=\infty$. Our primary observations are as follows:

- *In situ* oxygen plasma cleaning lowered the resistance of Ru contacts by two or more orders of magnitude,

but not lower than Au contacts, irrespective of whether the Au contacts were cleaned.
- Time-dependent creep properties of mixed Au-Ru contacts were observed to be similar to those of Au-Au contacts, the softer of the two materials.
- The absolute value of the resistance of mixed Au-Ru contacts was similar to that Ru-Ru contacts, the higher resistance material.
- Prior to, and for short oxygen plasma exposure times, bulk RuO_2 resistance values exhibited much larger variations than values measured for surface RuO_2, attributable to a higher degree of susceptibility to physisorbed hydrocarbons that are not removed by vacuum conditions (10^{-8} Torr) alone.
- For O_2 plasma exposure times exceeding about 5 min, the bulk and surface RuO_2 resistance values converged, at both $t=0$ and $t=\infty$, with the $t=\infty$ values falling within experimental error of theoretical values predicted for ideal surfaces, strongly suggesting that oxygen plasma both removes hydrocarbon contaminants and induces thickening of oxide layers on the Ru surfaces.
- The contact resistance of switches left open for eight days in a vacuum of 10^{-8} Torr was substantially higher than values measured immediately after cleaning, thus indicating that vacuum alone does not prevent contaminants from reforming after oxygen plasma exposure.

ACKNOWLEDGMENTS

This work was supported by AFOSR MURI under Grant No. FA9550-04-1-0381 entitled "Multifunctional Extreme Environment Surfaces: Nanotribology for Air and Space" and DARPA S&T Fundamentals Program, "Center for rf MEMS Reliability and Design Fundamentals," Grant No. HR0011-06-1-0051. The authors would also like to thank Dr. Z. J. Guo for assistance in sample preparation at Northeastern University. Sandia is a multiprogram laboratory operated by Sandia Corporation, a Lockheed Martin Co., for the United States Department of Energy's National Nuclear Security Administration under Contract No. DE-AC04-94AL85000.

[1]G. M. Rebeiz, *RF MEMS: Theory, Design, and Technology* (Wiley, New York, 2003).
[2]Z. J. Yao, S. Chen, S. Eshelman, D. Denniston, and C. Goldsmith, J. Microelectromech. Syst. **8**, 129 (1999).
[3]S. T. Patton and J. S. Zabinski, Tribol. Lett. **19**, 265 (2005).
[4]B. D. Jensen, L. L. W. Chow, K. W. Huang, K. Saitou, J. L. Volakis, and K. Kurabayashi, J. Microelectromech. Syst. **14**, 935 (2005).
[5]D. J. Dickrell III and M. T. Dugger, J. Microelectromech. Syst. **16**, 24 (2007).
[6]D. J. Dickrell III and M. T. Dugger, IEEE Trans. Compon. Packag. Technol. **30**, 75 (2007).
[7]C. Brown, A. S. Morris, A. I. Kingon, and J. Krim, J. Microeletromech. Syst. **17**, 1460 (2008).
[8]C. Brown, O. Rezvanian, M. A. Zikry, and J. Krim, J. Micromech. Microeng. **19**, 025006 (2009).
[9]A. Fortini, M. I. Mendelev, S. Buldyrev, and D. Srolovitz, J. Appl. Phys. **104**, 074320 (2008).
[10]H. Lee, R. A. Coutu, S. Mall, and K. D. Leddy, J. Micromech. Microeng. **16**, 557 (2006).
[11]L. Chen, H. Lee, Z. J. Guo, N. E. McGruer, K. W. Gilbert, S. Mall, K. D. Leedy, and G. G. Adams, J. Appl. Phys. **102**, 074910 (2007).
[12]F. X. Ke, J. M. Miao, and J. Oberhammer, J. Microelectromech. Syst. **17**, 1447 (2008).
[13]J. Liu, J. Lei, N. Magtoto, S. Rudenja, M. Garza, and J. A. Kelber, J. Electrochem. Soc. **152**, G115 (2005).
[14]J. Lee, S. Min, and S. H. Choh, J. Appl. Phys. **33**, 7080 (1994).
[15]Y. Iwasaki, A. Izumi, H. Tsurumaki, A. Namki, H. Oizumi, and I. Nishiyama, Appl. Surf. Sci. **253**, 8699 (2007).
[16]D. A. Hook, J. A. Olhausan, J. Krim, and M. T. Dugger, J. Microelectromech. Syst. (in press).
[17]O. Rezvanian, C. Brown, M. A. Zikry, A. I. Kingon, J. Krim, D. L. Irving, and D. W. Brenner, J. Appl. Phys. **104**, 024513 (2008).
[18]G. Wexler, Proc. Phys. Soc. **89**, 927 (1966).
[19]B. Nikolić and P. B. Allen, Phys. Rev. B **60**, 3963 (1999).
[20]N. Ashcroft, N. Mermin, and D. Mermin, *Solid State Physics*, 1st ed. (Holt, Rinehart and Winston, New York, 1976).
[21]S. Majumder, N. E. McGruer, G. G. Adams, P. M. Zavracky, R. H. Morrison, and J. Krim, Sens. Actuators, A **93**, 19 (2001).
[22]C. W. Dyck, T. A. Plut, C. D. Nordquist, P. S. Finnegan, F. Austin, I. Reines, and C. Goldsmith, SPIE Conference on Micromachining and Microfabrication, 2004, Vol. 5344, pp. 79–88.
[23]Keithely, 2400 Source Meter, www.keithley.com.
[24]Agilent, Model 33220A, www.agilent.com.
[25]TEGAM, Model 2350, www.tegam.com.
[26]Keithley, 2000 Multimeter, www.keithley.com.
[27]R. Holm, *Electric Contacts: Theory and Applications* (Springer, Berlin, Germany, 1969).
[28]B. Borovsky, J. Krim, S. A. Syed Asif, and K. J. Wahl, J. Appl. Phys. **90**, 6391 (2001).
[29]B. D. Dawson, S. M. Lee, and J. Krim, Phys. Rev. Lett. **103**, 205502 (2009).
[30]J. Krim, Amer. J. Phys. **70**, 890 (2001).
[31]J. Krim, Langmuir **12**, 4564 (1996).
[32]M. O. Robbins and J. Krim, MRS Bulletin **23**, 23 (1998).
[33]D. A. Hook, S. J. Timpe, M. T. Dugger, and J. Krim, J. Appl. Phys. **104**, 034303 (2008).
[34]J. H. Yoon, W. S. Lee, J. K. Park, G. W. Hwang, Y. J. Baik, T. Y. Seong, and J. H. Jeong, J. Appl. Phys. **107**, 044313 (2010).
[35]L. Wu, V. Rochus, L. Noels, and J. C. Golinval, J. Appl. Phys. **106**, 113502 (2009).
[36]J. Krim, I. Heyvaert, C. Van Haesendonck, and Y. Bruynseraede, Phys. Rev. Lett. **70**, 57 (1993).